

## Analysis of Order of Singularity at a Vertex in 3D Transversely Isotropic Piezoelectric Single-Step Bonded Joints

Md. Shahidul Islam, Md. Golam Kader, Md. Kamal Uddin, and Mohiuddin Ahmed

*Dept. of Mechanical Engineering, Khulna University of Engineering & Technology, Khulna, Bangladesh*

**Abstract:** - The stress singularity field occurs at a vertex on an interface due to a discontinuity of materials. The distribution of stress singularity field near the vertex of bonded joints is very important to maintain the reliability of intelligent materials. Piezoelectric materials are being widely used in the electronics industry, due to their high piezoelectric performance. Piezoelectric material, due to its characteristic direct-converse piezoelectric effect, has naturally received considerable attentions. In this paper, order of singularity at vertex in 3D transversely isotropic piezoelectric single-step bonded joints is analyzed. Eigen analysis based on FEM is used for stress singularity field analysis of piezoelectric bonded joints. The Eigen equation is used for calculating the order of stress singularity, and the angular function of elastic displacement, electric potential, stress and electric displacement. The numerical result shows that the angular functions have large value near the interface edge than the inner portion of the joint. From the numerical result, it was observed that the possibility of debonding at the interface edge of the piezoelectric bonded joints, due to the higher stress concentration at the free edge.

**Keywords:** - *Order of Singularity, Piezoelectric Single-step Joints, Transversely Isotropic material, Smart Structure, Finite Element Method.*

### I. INTRODUCTION

In recent years, intelligent or smart structures and systems have become an emerging new research area. Piezoelectric material, due to its characteristic direct-converse piezoelectric effect, has naturally received considerable attentions [1,2]. Piezoelectric materials have been extensively used as transducers and sensors due to their intrinsic direct and converse piezoelectric effects that take place between electric fields and mechanical deformation, and they are playing a key role as active components in many fields of engineering and technology such as electronics, laser, microwave infrared, navigation and biology [3]. For example, piezoelectric materials are acting as very important functional components in sonar projectors, fluid monitors, pulse generators and surface acoustic wave devices.

Mechanical stress occurs in piezoelectric material for any electric input. The stress concentrations caused by mechanical or electric loads may lead to crack initiation and extension, and sometimes the stress concentrations may be high enough to fracture the material parts. In the case of multilayer piezoelectric stacks, the electrodes that terminate inside the material body are a source of electric field, which can result in high stress concentrations. Reliable service lifetime predictions of piezoelectric components demand a complete understanding of the debonding processes of these materials. Industrial products such as electronic devices and heat endurance parts are composed of dissimilar materials. A mismatch of material properties causes a failure at the free edge of joint, because a stress concentration occurs along the free edge of interface especially at the vertex of bonded joint [4].

Sosa has suggested a general method of solving plane problems of piezoelectric media with defects [5]. Wang has obtained the general solutions of governing equations to three-dimensional axisymmetric problems in transversely isotropic piezoelectric media [6]. Williams used the mathematical procedure for analyzing stress singularities in infinite wedges and successfully applying to the analysis of stress distribution at the vicinity of a crack tip [7,8]. Zak and Williams used Eigen functions for analyzing stress singularity field at a crack tip perpendicular to a bimaterial interface [9]. They found that a real part of Eigen value is within the

range of 0 to 1, and expressed a relationship between stress distribution and the order of stress singularity at the crack tip. Aksentian determined Eigen values and Eigen vectors at the singular point in plane intersecting a free edge of the interface in three dimensional dissimilar joints [10].

Hartranft and Sih introduced the Eigen function expansions method in order to study the purely elastic 3D problem [11]. Bazent and Estenssoro, and Yamada and Okumura developed a finite element analysis for solving Eigen value equation to determine directly the order of stress singularity and the angular variation of the stress and displacement fields [12,13]. This Eigen analysis was used to evaluate the order of singularity at a point where a crack meets a free surface in an isotropic material. Then, this Eigen analysis based on a finite element was adapted by Pageau, Joseph and Biggers to use for analyzing the inplane deformation of wedges and junctions composed of anisotropic materials [14]. The stress and displacement fields were obtained from Eigen formulation for real and complex orders of stress singularity. Pageau and Biggers applied to analyze the joints including fully bonded multi-material junctions intersecting a free edge as well as materials containing crack intersecting a free edge [15]. This study showed that the order of singularity in the three-dimensional stress field could be accurately determined with a relatively small number of elements. Pageau and Biggers determined the order of stress singularity and the angular variation of the displacement and the stress fields around the singular points in plane intersecting a wedge front in the three-dimensional anisotropic material structures using the two dimensional displacement formulation under a plane strain assumption [16].

The effects of order of singularity near the vertex of 3D transversely isotropic piezoelectric bonded joints from a continuum mechanics point of view are not clear until now. Therefore, the effect of stress singularity field at a vertex on an interface of transversely isotropic piezoelectric single-step bonded joints is analyzed in this present study.

## II. THE GOVERNING EQUATION

In the absence of body forces and free charges, the equilibrium equations of piezoelectric materials are expressed as follows [17]:

$$\sigma_{ij,j} = 0, \quad d_{i,i} = 0 \tag{1}$$

The constitutive relations are shown as follows:

$$\sigma_{ij} = c_{ijkl} \varepsilon_{kl} - e_{kij} E_k, \quad d_i = e_{ikl} \varepsilon_{kl} - \chi_{ik} E_k \tag{2}$$

The elastic strain-displacement and electric field-potential relations are presented as follows:

$$\varepsilon_{ij} = \frac{1}{2}(u_{j,i} + u_{i,j}), \quad E_i = -\psi_{,i} \tag{3}$$

where  $i, j, k, l = 1, 2, 3$  and  $\sigma_{ij}, d_i, \varepsilon_{ij}, u_i, E_i,$  and  $\psi$  are the component of stress, electric displacement, strain, elastic displacement, electric field and electric potential respectively. Eq. (2) expressed in terms of elastic stiffness constant  $c_{ijkl}$  (measured in a constant electric field), the piezoelectric constant  $e_{ikl}$  and electric permittivity (dielectric constant)  $\chi_{ik}$  (measured at a constant strain).

For transversely isotropic material, taking  $z$ -axis parallel to the poling axis of the material, by convention, the constructive relation is expressed in the following form.

$$\{\sigma\} = [c]\{\varepsilon\} - [e]\{E\}, \quad \{d\} = [e]^T \{\varepsilon\} - [\chi]\{E\} \tag{4}$$

where  $\{\sigma\}$  and  $\{\varepsilon\}$  are the stress and strain which are the mechanical field variables,  $\{d\}$  and  $\{E\}$  are the electric displacement and electric field respectively,  $[c]$  is the elastic constant, and  $[e]$  and  $[\chi]$  are the piezoelectric and electric permittivity (dielectric) constant respectively.

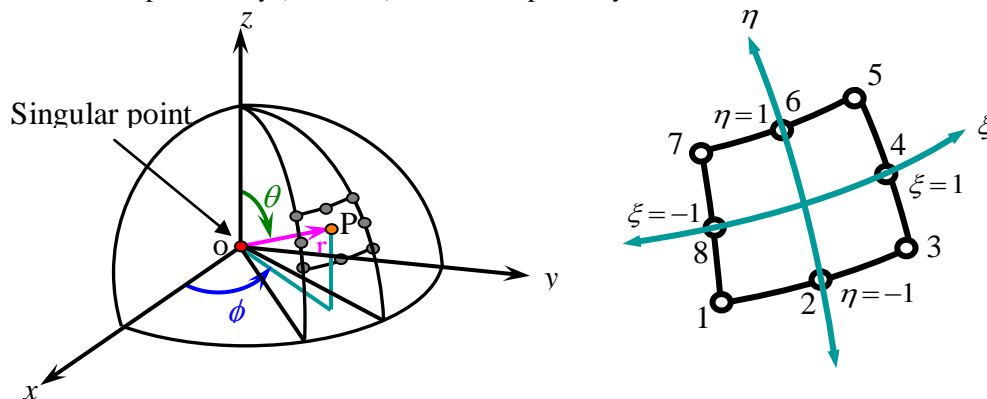


Figure 1: Element geometry and natural co-ordinates at a free edge singular point

Fig. 1 represents the geometry of a typical case where a singular stress state occurs at the point o. The region surrounding the singular point is divided into a number of quadratic pyramidal elements with a summit o, with each element being located in spherical coordinates  $r$ ,  $\theta$ , and  $\phi$  by its nodes 1 to 8. A point P in the element can be located using the singular transformation by the following relations.

$$r = r_o \left( \frac{1 + \alpha}{2} \right)^{1/p} \quad \text{or,} \quad \rho = \frac{r}{r_o} = \left( \frac{1 + \alpha}{2} \right)^{1/p} \tag{5}$$

$$\theta = \sum_{i=1}^8 H_i \theta_i \quad \text{and} \quad \phi = \sum_{i=1}^8 H_i \phi_i \tag{6}$$

where  $p$  Eigen value,  $\rho = r/r_o$ ,  $r$  the distance from the singular point, and  $H_i$  indicates the shape function, which is written as;

$$\begin{aligned} H_1 &= -\frac{1}{4}(1-\eta)(1-\xi)(\eta+\xi+1) & H_2 &= \frac{1}{2}(1-\eta)(1-\xi^2) \\ H_3 &= -\frac{1}{4}(1-\eta)(1+\xi)(-\eta+\xi-1) & H_4 &= \frac{1}{2}(1-\eta^2)(1+\xi) \\ H_5 &= \frac{1}{4}(1+\eta)(1+\xi)(\eta+\xi-1) & H_6 &= \frac{1}{2}(1+\eta)(1-\xi^2) \\ H_7 &= \frac{1}{4}(1+\eta)(1-\xi)(\eta-\xi-1) & H_8 &= \frac{1}{2}(1-\eta^2)(1-\xi) \end{aligned} \tag{7}$$

$\theta$  and  $\phi$  are the nodal values of the angular coordinates and  $\alpha$ ,  $\eta$ , and  $\xi$  are natural coordinates of the element whose ranges are shown in Fig.1.

The elastic displacement and electric potential field in the element is expressed as follows:

$$\left( \bar{u} - \bar{u}_o \right) = \left( \frac{1 + \alpha}{2} \right) \left[ \sum_{i=1}^8 H_i \left( \bar{u}_i - \bar{u}_o \right) \right], \quad \text{and} \quad \left( \bar{\psi} - \bar{\psi}_o \right) = \left( \frac{1 + \alpha}{2} \right) \left[ \sum_{i=1}^8 H_i \left( \bar{\psi}_i - \bar{\psi}_o \right) \right] \tag{8}$$

where  $\bar{u}_o$  and  $\bar{u}$  represents the elastic displacement vector of the vertex o and the point P respectively, and  $\bar{u}_i$  represents the elastic displacement vector of the node  $i$  ( $i = 1, 2, \dots, 8$ ). Similarly  $\bar{\psi}_o$  and  $\bar{\psi}$  represents the electric potential vector of the vertex o and the point P respectively, and  $\bar{\psi}_i$  represents the electric potential vector of the node  $i$  ( $i = 1, 2, \dots, 8$ ). In order to simplify the notation, the following equation can be defined.

$$u = \left( \bar{u} - \bar{u}_o \right), \quad u_i = \left( \bar{u}_i - \bar{u}_o \right), \quad \text{and} \quad \psi = \left( \bar{\psi} - \bar{\psi}_o \right), \quad \psi_i = \left( \bar{\psi}_i - \bar{\psi}_o \right) \tag{9}$$

Using the Eq. (5), Eq. (8) can be expressed as follows:

$$u_k = \rho^p \left[ \sum_{i=1}^8 H_i u_{ki} \right] \quad (k = r, \theta, \phi), \quad \text{and} \quad \psi = \rho^p \left[ \sum_{i=1}^8 H_i \psi_i \right] \tag{10}$$

The Jacobean matrix relating the spherical coordinates to the natural coordinates is given below:

$$[J] = \begin{bmatrix} \frac{\partial r}{\partial \alpha} & \frac{\partial \theta}{\partial \alpha} & \frac{\partial \phi}{\partial \alpha} \\ \frac{\partial r}{\partial \xi} & \frac{\partial \theta}{\partial \xi} & \frac{\partial \phi}{\partial \xi} \\ \frac{\partial r}{\partial \eta} & \frac{\partial \theta}{\partial \eta} & \frac{\partial \phi}{\partial \eta} \end{bmatrix} = \begin{bmatrix} \frac{r_o}{2p} \rho^{1-p} & 0 & 0 \\ 0 & \sum_{i=1}^8 H_{i,\xi} \theta_i & \sum_{i=1}^8 H_{i,\xi} \phi_i \\ 0 & \sum_{i=1}^8 H_{i,\eta} \theta_i & \sum_{i=1}^8 H_{i,\eta} \phi_i \end{bmatrix} \quad (11)$$

Eq. (11) shows that there is no dependence between the radial coordinate and the angular coordinate. From Eq. (11) a sub-matrix is extracted as follows:

$$[J_1] = \begin{bmatrix} \frac{\partial \theta}{\partial \xi} & \frac{\partial \phi}{\partial \xi} \\ \frac{\partial \theta}{\partial \eta} & \frac{\partial \phi}{\partial \eta} \end{bmatrix} = \begin{bmatrix} \sum_{i=1}^8 H_{i,\xi} \theta_i & \sum_{i=1}^8 H_{i,\xi} \phi_i \\ \sum_{i=1}^8 H_{i,\eta} \theta_i & \sum_{i=1}^8 H_{i,\eta} \phi_i \end{bmatrix} \quad (12)$$

The strain and electric potential equation is obtained from Eq. (5)~ Eq. (7) and Eq. (10), Eq. (12) by using the chain rule of differentiation.

The strain in a spherical coordinate system:

$$\begin{aligned} \epsilon_{rr} &= \frac{\partial u_r}{\partial r} = \frac{p\rho^{p\lambda-1}}{r_o} \left[ \sum_{i=1}^8 H_i u_{ri} \right] \\ \epsilon_{\theta\theta} &= \frac{\partial u_\theta}{r \partial \theta} + \frac{u_r}{r} = \left( \frac{\rho^{p-1}}{r_o} \right) \left\{ \sum_{i=1}^8 H_i u_{ri} + [J_1(1,1)]^{-1} \left[ \sum_{i=1}^8 \frac{\partial H_i}{\partial \xi} u_{\theta i} \right] + [J_1(1,2)]^{-1} \left[ \sum_{i=1}^8 \frac{\partial H_i}{\partial \eta} u_{\theta i} \right] \right\} \\ \epsilon_{\phi\phi} &= \frac{u_\theta}{r} \cot \theta + \frac{1}{r \sin \theta} \frac{\partial u_\phi}{\partial \phi} + \frac{u_r}{r} = \left( \frac{\rho^{p-1}}{r_o} \right) \left\{ \sum_{i=1}^8 H_i u_{ri} + \cot \theta \left[ \sum_{i=1}^8 H_i u_{\theta i} \right] \right. \\ &\quad \left. + \frac{[J_1(2,1)]^{-1}}{\sin \theta} \left[ \sum_{i=1}^8 \frac{\partial H_i}{\partial \xi} u_{\phi i} \right] + \frac{[J_1(2,2)]^{-1}}{\sin \theta} \left[ \sum_{i=1}^8 \frac{\partial H_i}{\partial \eta} u_{\phi i} \right] \right\} \\ \gamma_{\theta\phi} &= \frac{1}{r \sin \theta} \frac{\partial u_\theta}{\partial \phi} + \frac{\partial u_\phi}{r \partial \theta} - \frac{u_\phi}{r} \cot \theta \\ &= \left( \frac{\rho^{p-1}}{r_o} \right) \left\{ -\cot \theta \left[ \sum_{i=1}^8 H_i u_{\phi i} \right] + [J_1(1,1)]^{-1} \left[ \sum_{i=1}^8 \frac{\partial H_i}{\partial \xi} u_{\phi i} \right] + [J_1(1,2)]^{-1} \left[ \sum_{i=1}^8 \frac{\partial H_i}{\partial \eta} u_{\phi i} \right] \right. \\ &\quad \left. + \frac{[J_1(2,1)]^{-1}}{\sin \theta} \left[ \sum_{i=1}^8 \frac{\partial H_i}{\partial \xi} u_{\theta i} \right] + \frac{[J_1(2,2)]^{-1}}{\sin \theta} \left[ \sum_{i=1}^8 \frac{\partial H_i}{\partial \eta} u_{\theta i} \right] \right\} \\ \gamma_{r\phi} &= \frac{1}{r \sin \theta} \frac{\partial u_r}{\partial \phi} + \frac{\partial u_\phi}{\partial r} - \frac{u_\phi}{r} = \left( \frac{\rho^{p-1}}{r_o} \right) \left\{ (p-1) \left[ \sum_{i=1}^8 H_i u_{\phi i} \right] \right. \\ &\quad \left. + \frac{[J_1(2,1)]^{-1}}{\sin \theta} \left[ \sum_{i=1}^8 \frac{\partial H_i}{\partial \xi} u_{ri} \right] + \frac{[J_1(2,2)]^{-1}}{\sin \theta} \left[ \sum_{i=1}^8 \frac{\partial H_i}{\partial \eta} u_{ri} \right] \right\} \\ \gamma_{r\theta} &= \frac{\partial u_r}{r \partial \theta} + \frac{\partial u_\theta}{\partial r} - \frac{u_\theta}{r} = \left( \frac{\rho^{p-1}}{r_o} \right) \left\{ (p-1) \left[ \sum_{i=1}^8 H_i u_{\theta i} \right] \right\} \end{aligned}$$

$$+ [J_1(1,1)]^{-1} \left[ \sum_{i=1}^8 \frac{\partial H_i}{\partial \xi} u_{ri} \right] + [J_1(1,2)]^{-1} \left[ \sum_{i=1}^8 \frac{\partial H_i}{\partial \eta} u_{ri} \right] \} \tag{13}$$

The electric potential in a spherical coordinate system:

$$E_r = -\frac{\partial \psi}{\partial r} = -\left( \frac{\rho \rho^{p-1}}{r_o} \right) \left[ \sum_{i=1}^8 H_i \psi_i \right]$$

$$E_\theta = -\frac{\partial \psi}{r \partial \theta} = -\left( \frac{\rho^{p-1}}{r_o} \right) \left\{ [J_1(1,1)]^{-1} \left[ \sum_{i=1}^8 \frac{\partial H_i}{\partial \xi} \psi_i \right] + [J_1(1,2)]^{-1} \left[ \sum_{i=1}^8 \frac{\partial H_i}{\partial \eta} \psi_i \right] \right\}$$

$$E_\phi = -\frac{1}{r \sin \theta} \frac{\partial \psi}{\partial \phi} = -\left( \frac{\rho^{p-1}}{r_o} \right) \left\{ \frac{[J_1(2,1)]^{-1}}{\sin \theta} \left[ \sum_{i=1}^8 \frac{\partial H_i}{\partial \xi} \psi_i \right] + \frac{[J_1(2,2)]^{-1}}{\sin \theta} \left[ \sum_{i=1}^8 \frac{\partial H_i}{\partial \eta} \psi_i \right] \right\} \tag{14}$$

The superscript -1 on the matrix  $[J_1]$  represents the inverse matrix. Eq. (13) and Eq. (14) now can be summarized as follows:

$$\{\boldsymbol{\varepsilon}^*\} = \sum_{i=1}^8 [\mathbf{B}_i] \{\mathbf{u}_i^*\} = [\mathbf{B}] \{\mathbf{u}^*\} \tag{15}$$

where  $\{\boldsymbol{\varepsilon}^*\}^T = \{\varepsilon_{rr} \quad \varepsilon_{\theta\theta} \quad \varepsilon_{\phi\phi} \quad \varepsilon_{r\theta} \quad \varepsilon_{r\phi} \quad \varepsilon_{\theta\phi} \quad E_r \quad E_\theta \quad E_\phi\}$

$$\{\mathbf{u}_i^*\}^T = \{\bar{u}_{ri} \quad \bar{u}_{\theta i} \quad \bar{u}_{\phi i} \quad -\bar{\psi}_i\}$$

$$[\mathbf{B}] = \frac{1}{r_o} \rho^{p-1} (p [\mathbf{B}_a] + [\mathbf{B}_b])$$

$$[\mathbf{B}_{ia}] = \begin{bmatrix} H_i & 0 & 0 & 0 \\ 0 & 0 & 0 & 0 \\ 0 & 0 & 0 & 0 \\ 0 & H_i & 0 & 0 \\ 0 & 0 & H_i & 0 \\ 0 & 0 & 0 & 0 \\ 0 & 0 & 0 & H_i \\ 0 & 0 & 0 & 0 \\ 0 & 0 & 0 & 0 \end{bmatrix}, \text{ and } [\mathbf{B}_{ib}] = \begin{bmatrix} 0 & 0 & 0 & 0 \\ H_i & A_1 & 0 & 0 \\ H_i & H_i \cot \theta & A_2 & 0 \\ A_1 & -H_i & 0 & 0 \\ A_2 & 0 & -H_i & 0 \\ 0 & A_2 & A_1 - H_i \cot \theta & 0 \\ 0 & 0 & 0 & 0 \\ 0 & 0 & 0 & A_1 \\ 0 & 0 & 0 & A_2 \end{bmatrix} \tag{16}$$

Also  $A_1$  and  $A_2$  are written as;

$$A_1 = [J_1(1,1)]^{-1} \left[ \frac{\partial H_i}{\partial \xi} \right] + [J_1(1,2)]^{-1} \left[ \frac{\partial H_i}{\partial \eta} \right], \text{ and } A_2 = \frac{[J_1(2,1)]^{-1}}{\sin \theta} \left[ \frac{\partial H_i}{\partial \xi} \right] + \frac{[J_1(2,2)]^{-1}}{\sin \theta} \left[ \frac{\partial H_i}{\partial \eta} \right] \tag{17}$$

Eq. (15) ~ Eq. (17) represents the strains, and therefore the stresses are proportional to  $\rho^{p-1}$ . The case where  $0 < p < 1$  defines a singular stress state at the vertex of the element. The element depicted in Fig.1 must satisfy the principle of virtual work in order to be in equilibrium, that is

$$\int_{\Omega} \sigma_{ij}^* \delta \varepsilon_{ij}^* d\Omega = \int_{\Gamma} T_i^* \delta u_i^* d\Gamma + \int_{\Omega} f_i^* \delta u_i^* d\Omega \tag{18}$$

Where  $T_i^*$  represents the traction at the outer boundary. This equation can be transformed into a matrix form with the help of Eq. (5)~ Eq. (7) as follows:

$$\int_{-1}^1 \int_{-1}^1 \int_{-1}^1 r_o^2 \rho^2 \left( \delta \{ \varepsilon^* \}^T \{ \sigma^* \} \right) \sin \theta |J| d\alpha d\xi d\eta = \int_{-1}^1 \int_{-1}^1 r_o^2 \left( \delta \{ \mathbf{u}^* \}^T \{ \mathbf{H} \}^T \begin{Bmatrix} \sigma_{rr} \\ \sigma_{r\phi} \\ \sigma_{r\theta} \\ d_r \end{Bmatrix} \right) \sin \theta |J_1| d\xi d\eta \tag{19}$$

where  $|J|$  and  $|J_1|$  represent the determinant of the matrices  $[J]$  and  $[J_1]$  respectively and  $\{ \sigma^* \}^T$  is represented by the following equation.

$$\{ \sigma^* \}^T = \{ \sigma_{rr} \quad \sigma_{\theta\theta} \quad \sigma_{\phi\phi} \quad \tau_{r\theta} \quad \tau_{r\phi} \quad \tau_{\theta\phi} \quad d_r \quad d_{\theta} \quad d_{\phi} \} \tag{20}$$

The relation between stress and electric displacement with strain and electric field is as follows:

$$\{ \sigma^* \} = [D] \{ \varepsilon^* \} \tag{21}$$

where  $[D]$  represents the material constants matrix.

The Eigen equation was formulated for determining the order of stress singularity as follows [14]:

$$(p^2 [A] + p [B] + [C]) \{ U \} = \{ 0 \} \tag{22}$$

where

$$\{ U \} = \begin{Bmatrix} u_r \\ u_{\theta} \\ u_{\phi} \\ \psi \end{Bmatrix}, \text{ and}$$

$$[A] = \sum_S ([k_a - k_{sa}]), \quad [B] = \sum_S ([k_b - k_{sb}]), \quad [C] = \sum_S ([k_c - k_{sc}])$$

In Eq. (22),  $p$  represents the characteristic root, which is related to the order of singularity,  $\lambda$ , as  $\lambda = 1-p$ .  $[A]$ ,  $[B]$  and  $[C]$  are matrices composed of material properties, and  $\{U\}$  represents the elastic displacement and electric potential vector.

$$[k_a] = \int_{-1}^1 \int_{-1}^1 [B_a]^T [D] [B_a] \sin \theta |J_1| d\xi d\eta$$

$$[k_b] = \int_{-1}^1 \int_{-1}^1 \left( [B_a]^T [D] [B_b] + [B_b]^T [D] [B_a] \right) \sin \theta |J_1| d\xi d\eta$$

$$[k_c] = \int_{-1}^1 \int_{-1}^1 [B_b]^T [D] [B_b] \sin \theta |J_1| d\xi d\eta$$

$$[k_{sa}] = 2 \int_{-1}^1 \int_{-1}^1 [H]^T [SD] [B_a] \sin \theta |J_1| d\xi d\eta$$

$$[k_{sb}] = \int_{-1}^1 \int_{-1}^1 (2[H]^T [SD][B_b] + [H]^T [SD][B_a]) \sin \theta |J_1| d\xi d\eta$$

$$[k_{sc}] = \int_{-1}^1 \int_{-1}^1 [H]^T [SD][B_b] \sin \theta |J_1| d\xi d\eta$$

Eq. (22) now expressed as follows

$$(-p[B] - [C])\{U\} = p^2 [A]\{U\} \tag{23}$$

Finally, letting  $\{V\} = p\{U\}$ , the characteristic equation can be transformed into the standard Eigen problem.

$$\begin{bmatrix} -[A]^{-1}[B] & -[A]^{-1}[C] \\ [I] & [0] \end{bmatrix} \begin{Bmatrix} \{V\} \\ \{U\} \end{Bmatrix} = p \begin{Bmatrix} \{V\} \\ \{U\} \end{Bmatrix} \tag{24}$$

### III. RESULTS AND DISCUSSIONS

Fig. 2 represents a model for 3D two-phase transversely isotropic piezoelectric dissimilar joints used in the present analysis. The stress singularity line and singularity point on interface of the joint are shown in the figure. The angle  $\theta$  is equal to  $180^\circ$  and the angle  $\phi$  for upper material and lower material are  $90^\circ$  and  $360^\circ$  respectively. In Eigen analysis, a mesh division for the joint is needed for the analysis. The mesh developed on  $\phi-\theta$  plane is shown in Fig. 3, where the surface of a unit sphere is divided into  $\phi \times \theta = 10^\circ \times 10^\circ$ .

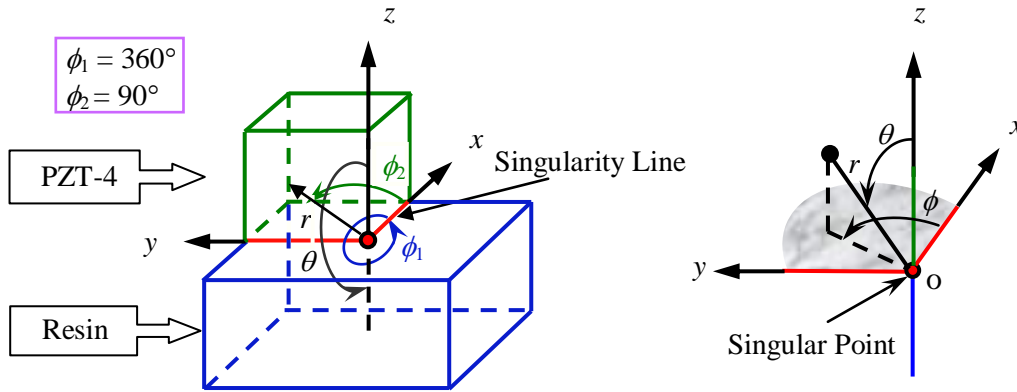


Figure 2: Singular point of 3D piezoelectric single-step bonded joint in x, y, z plane

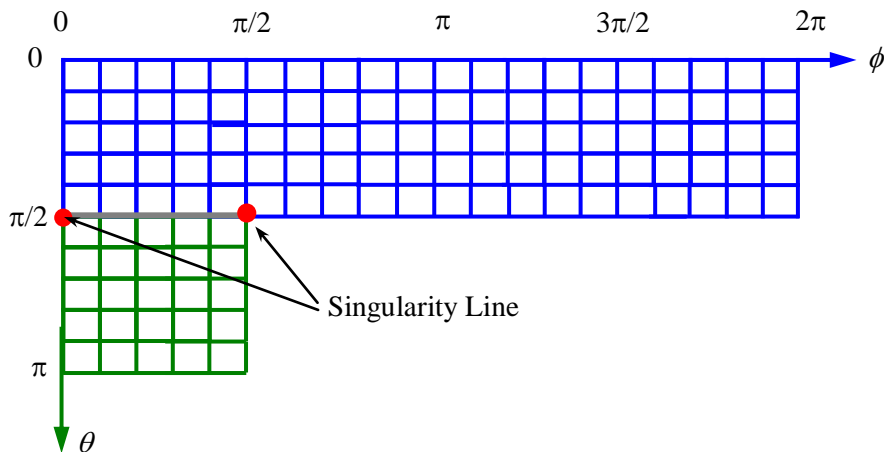


Figure 3: A mesh on developed  $\phi-\theta$  plane

Table 1. Material properties of piezoelectric materials

Material	Elastic Constant, $10^{10}$ N/m <sup>2</sup>					Piezoelectric Constant, C/m <sup>2</sup>			Dielectric Constant, $10^{-10}$ C/Vm	
	$c_{11}$	$c_{12}$	$c_{13}$	$c_{33}$	$c_{44}$	$e_{31}$	$e_{33}$	$e_{15}$	$\chi_{11}$	$\chi_{33}$
Resin	5.56	3.41	3.41	5.56	1.08	0.0	0.0	0.0	37.9	37.9
PZT-4	13.9	7.78	7.43	11.3	2.56	-6.98	13.8	13.4	60.0	54.7

In this analysis, first of all, Eigen values and Eigen vectors are investigated by Eigen analysis when two different materials are bonded. The order of singularity  $\lambda$ , at the vertex and at a point on the singularity line for the model shown in Fig. 2 is calculated. Solving Eigen equation yields many roots  $p$  and Eigen vectors corresponding to each Eigen value are obtained. However, if the root  $p$  is within the range of  $0 < p < 1$ , this fact indicates that the stress field has singularity. The values of the order of singularity at the singularity corner and line for transversely isotropic piezoelectric bonded material are shown in Table 2.

Table 2. Order of singularity for Resin and PZT-4

Material	Order of singularity				
	$\lambda$	1	2	3	4
PZT-4 and Resin	$\lambda_{line}$	0.3494	0.0895	0.0264	----
	$\lambda_{vertex}$	0.4304	0.0291	0.0081	0.0023

The angular functions of elastic displacement and electric potential equation are expressed by the following equation.

$$u_j(r, \theta, \phi) = b_j(\theta, \phi)r^{1-\lambda}, \text{ and } \psi(r, \theta, \phi) = q(\theta, \phi)r^{1-\lambda} \quad (j = r, \theta, \phi) \quad (25)$$

By differentiating the above equations, get the angular function of strain and electric field equation respectively. The stress and electric displacement distribution equations in the stress singularity region can be expressed as follows.

$$\sigma_{ij}(r, \theta, \phi) = K_{ij}r^{-\lambda}f_{ij}(\theta, \phi), \text{ and } d_i(r, \theta, \phi) = F_i r^{-\lambda}l_i(\theta, \phi) \quad (i, j = r, \theta, \phi) \quad (26)$$

Where  $r$  represents the distance from the stress singular point,  $b_j(\theta, \phi)$  the angular function of elastic displacement,  $q(\theta, \phi)$  the angular function of electric potential,  $f_{ij}(\theta, \phi)$  the angular function of stress distribution,  $l_i(\theta, \phi)$  the angular function of electric displacement,  $K_{ij}$  the intensity of singularity,  $F_i$  the intensity of electric field, and  $\lambda$  the order of stress singularity. Angular functions of stress components obtained from Eigen analysis in Eq. (22) are examined.

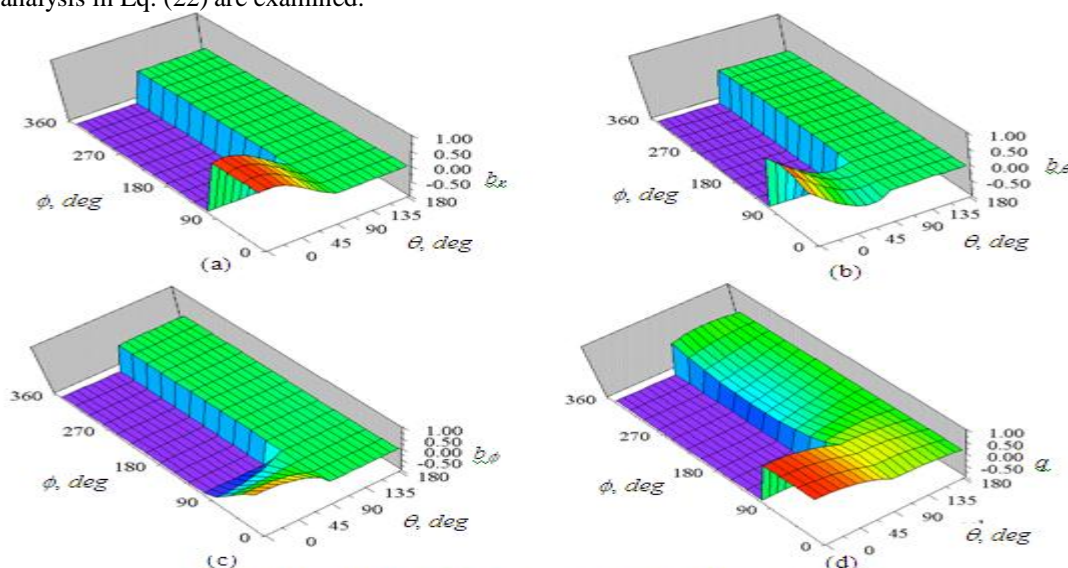


Figure 4: Distribution of  $b$ , and  $q$  against  $\phi$  &  $\theta$  for Resin & PZT-4

Fig. 4 shows the distribution of angular function of elastic displacement and electric potential at  $\lambda_1 = 0.4304$ . Plots (a), (b) and (c) represent the elastic displacement and plot (d) represent the electric potential. All figures are plotted by using the Eq. (25). All of these plots show that the angular functions are continuous at the interface of the bonded joint. The interface of the joint is at  $\theta = 90^\circ$ . Resin is exist in the region of  $\phi = 0^\circ$  to  $360^\circ$ ,  $\theta = 90^\circ$  to  $180^\circ$  and PZT-4 is exist in the region of  $\phi = 0^\circ$  to  $90^\circ$ ,  $\theta = 0^\circ$  to  $90^\circ$ . The distribution of angular function of stress against  $\phi$  and  $\theta$  for  $\lambda = 0.4304$  is plotted by using the Eq. (26) and the graphs are shown in the figure below:

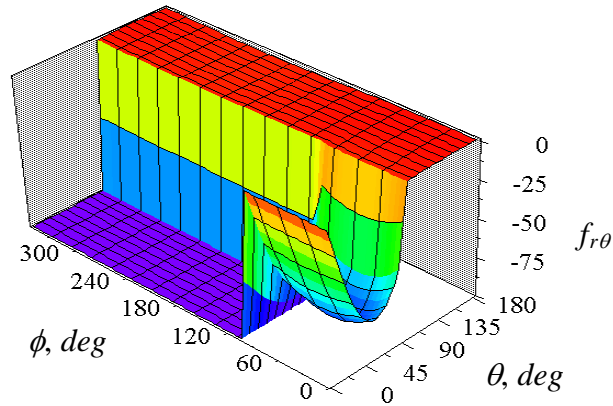


Figure 5: Distribution of  $f_{r\theta}$  against  $\phi$  and  $\theta$  for Resin & PZT-4

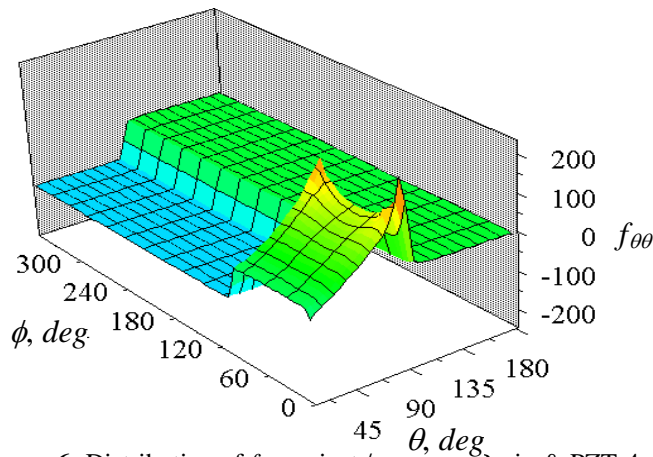


Figure 6: Distribution of  $f_{\theta\theta}$  against  $\phi$  and  $\theta$  for Resin & PZT-4

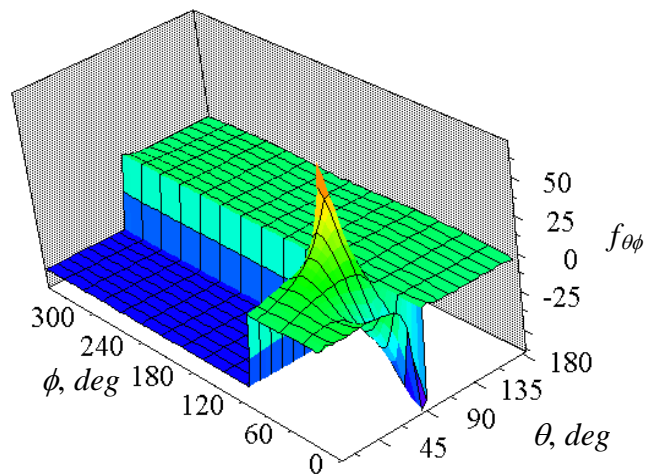


Figure 7: Distribution of  $f_{\theta\phi}$  against  $\phi$  and  $\theta$  for Resin & PZT-4

Fig. 5~7 show the 3D distribution of angular function of stress in  $\phi$ - $\theta$  plane for  $\lambda = 0.4304$ . All these graphs show the angular function of stress have the larger value at the interface edge of the bonded joint. The distribution of angular function of electric displacement against  $\phi$  and  $\theta$  for  $\lambda = 0.4304$  is plotted by using the Eq. (26) and the graphs are shown in the figure below:

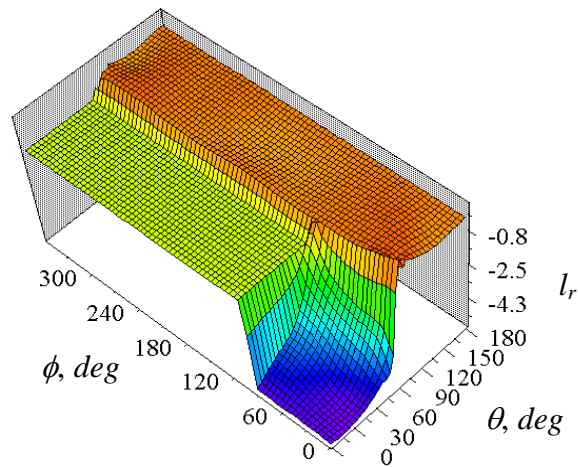


Figure 8: Distribution of  $l_r$  against  $\phi$  and  $\theta$  for Resin & PZT-4

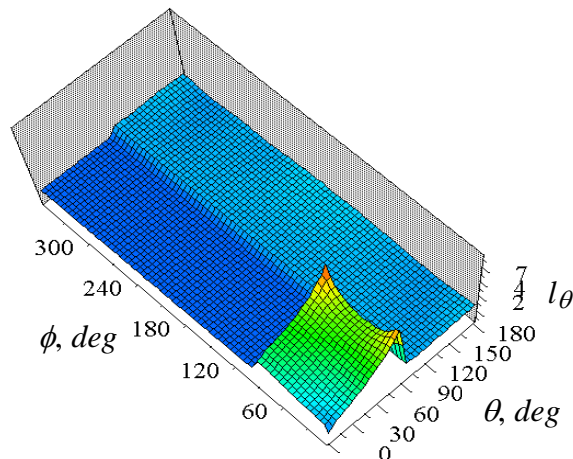


Figure 9: Distribution of  $l_\theta$  against  $\phi$  and  $\theta$  for Resin & PZT-4

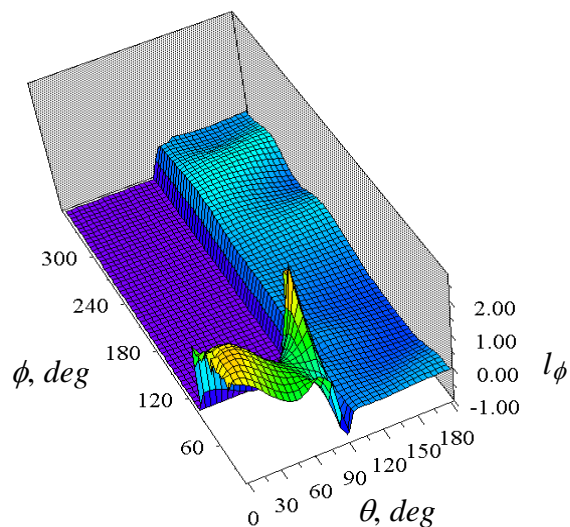
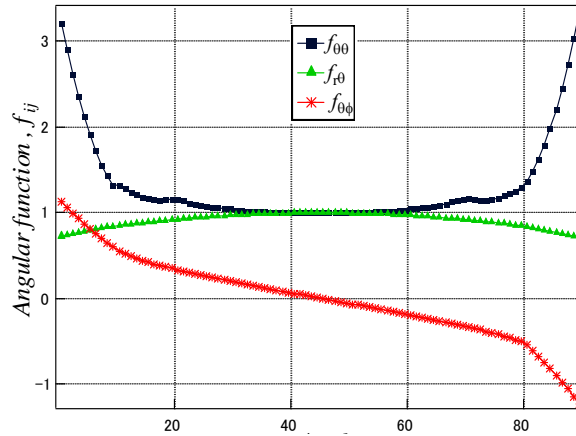


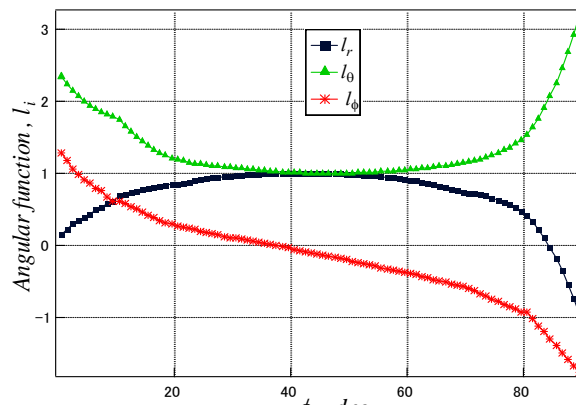
Figure 10: Distribution of  $l_\phi$  against  $\phi$  and  $\theta$  for Resin & PZT-4

Fig. 8~10 show the 3D distribution of angular function of electric displacement in  $\phi$ - $\theta$  plane for  $\lambda = 0.4304$ . All these figures show the angular function of electric displacement is continuous at the interface of the bonded joint. These figures also show that the larger value of angular function of electric displacement near the interface edge than the in



**Figure11:** Distribution of normalized  $f_{ij}$  against  $\phi$  at  $\theta = 90^\circ$  for Resin & PZT-4

The normalized angular function of stress is shown in Fig. 11 for  $\lambda = 0.4304$ . The angular function of stress against the angle  $\phi$  at  $\theta = 90^\circ$  is plotted. The stress singularity lines are at the free edge of the material joint. The figure shows that the value of angular function of stress increases rapidly near the interface edge than the inner portion of the joints. The values of  $f_{r\theta}$  and  $f_{\theta\theta}$  is normalized by their value at  $\phi = 45^\circ$  and  $f_{\phi\theta}$  is normalized by their value at  $\phi = 2.5^\circ$ . Near interface edge of the joint has the largest value of angular function of stress. So there is a possibility to debond and delamination occurs near the interface edge of the single-step bonded joint.



**Figure12:** Distribution of normalized  $l_i$  against  $\phi$  at  $\theta = 90^\circ$  for Resin & PZT-4

The normalized angular function of electric displacement is shown in Fig. 12 for  $\lambda = 0.4304$ . The angular function of electric displacement against the angle  $\phi$  at  $\theta = 90^\circ$  is plotted. This figure also shows that the value of angular function of electric displacement increases rapidly near the free edge than the inner portion of the joints. The value of  $l_r$  and  $l_\theta$  is normalized by their value at  $\phi = 45^\circ$  and  $l_\phi$  is normalized by their value at  $\phi = 3.5^\circ$ . The angular function of electric displacement has the larger value near the interface edge than the inner portion of the joint. So there is another possibility to debond and delamination occurs near the interface edge of the single-step bonded joint.

#### IV. CONCLUSIONS

An Eigen equation formulation near the vertex of transversely isotropic piezoelectric single-step bonded joint was presented. Angular functions for singularity corner were derived from Eigen analysis based on

a finite element method. From the numerical results, the following conclusions can be drawn for the piezoelectric single-step bonded joints.

(a) The order of singularity at the singularity corner is larger than that of the line.

(b) Larger value of the angular function occurs at the interface edge in the material joint than the inner portion of the joint.

(c) It is suggested that delamination of the interface may occur at the interface edge of the piezoelectric material joints.

## V. ACKNOWLEDGMENTS

I would like to express my deep and sincere gratitude to Prof. Hideo Koguchi, Nagaoka University of Technology, Japan. I am deeply grateful to Takahiko Kurahashi, Nagaoka University of Technology, Japan for his detailed and constructive comments throughout this work.

### Notations

$\sigma_{ij}$	Stress, N/m <sup>2</sup>
$\epsilon_{ij}$	Strain, m/m
$d_i$	Electric displacement, C/m <sup>2</sup>
$E_i$	Electric field, N/C
$c_{ijkl}$	Elastic constant, N/m <sup>2</sup>
$e_{ikl}$ ( $e_{kij}$ )	Piezoelectric constant, C/m <sup>2</sup>
$\chi_{ik}$	Electric permittivity, C <sup>2</sup> /Nm <sup>2</sup>
$H$	Interpolation function
$p$	Characteristic root
$\lambda$	Order of singularity
$u_i$	Elastic displacement
$\psi$	Electric potential

## REFERENCES

- [1] Ding, H. and Chenbuo, On the Green's functions for two-phase transversely isotropic piezoelectric media, *Int. J. of Solids and Structure*, 34(23), 3041-3057, 1997.
- [2] Ming, H. Z., Ping Z. F. and Ya P. S, Boundary integral-differential equations and boundary element method for interfacial cracks in three-dimensional piezoelectric media, *Engineering Analysis with Boundary Elements*, 28, 753-762, 2004.
- [3] Wang, Z. and Zheng, B., The general solution of three-dimensional problems in piezoelectric media, *Int. J. of Solids and Structure*, 32(1), 105-115, 1995.
- [4] Attaporn, W. and Koguchi, H., Intensity of stress singularity at a vertex and along the free edges of the interface in 3D-dissimilar material joints using 3D-enriched FEM, *CMES*, 39(3), 237-262, 2009.
- [5] Sosa, H. A., Plane problems in piezoelectric media with defects, *Int. J. of Solids and Structure*, 28, 491-505, 1991.
- [6] Wang, Z. K., Penny-shaped crack in transversely isotropic piezoelectric materials", *Acta Mechanica Sinica*, 10, 1-8, 1994.
- [7] Williams, M. L., Stress singularities resulting from various boundary conditions in angular corners of plates in extension, *ASME J. of Applied Mechanics*, 19, 526, 1952.
- [8] Williams, M. L., On the stress at the base of stationary crack", *ASME J. of Applied Mechanics*, 24, 109-114, 1957.
- [9] Zak, A. R. and Williams, M. L., Crack point stress singularities at a bi-material interface, *J. of Applied Mechanics, Brief Notes*, 142-143, 1963.
- [10] Aksentian, O. K., Singularities of the stress-strain state of a plate in the neighborhood of an edge, *PMM*, 31(1), 178-186, 1967.
- [11] Hartranft, R. J., and Sih, G. C., The use of Eigen function expansions I the general solution of three-dimensional crack problem, *J. of Mathematical Mechanics*, 19, 123-138, 1969.
- [12] Bazent, Z. P. and Estenssoro, L. F., Surface singularity and crack propagation, *Int. J. of Solids and Structure*, 15, 405-426, 1979.
- [13] Yamada, Y. and Okumura, H., Analysis of local stress in composite materials by 3-D finite element, *Proceeding of the Japan-U.S. Conference*, Tokyo, Japan, 55-64, 1981.
- [14] Pageau, S. S., Joseph, P. F. and Biggers, Jr. S. B., Finite element analysis of anisotropic materials with singular inplane stress fields, *Int. J. of Solids and Structure*, 32, 571-591, 1995.
- [15] Pageau, S. S. and Biggers, Jr. S. B., Finite element evaluation of free-edge singular stress fields in anisotropic materials", *Int. J. Numer. Methods in Engineering*, 38, 2225-2239, 1995.
- [16] Pageau, S. S. and Biggers, Jr. S. B., A finite element approach to three-dimensional singular stress states in anisotropic multi-material wedges and junctions, *Int. J. of Solids and Structure*, 33, 33-47, 1996.
- [17] Liew, K. M. and Liang, J., Modeling of 3D piezoelectric and elastic bimetals using the boundary element method, *Computational Mechanics*, 29, 151-162, 2002.
- [18] XU, J. Q., and Mutoh, Y., Singularity at the interface edge of bonded transversely isotropic piezoelectric dissimilar

- material, *JSME International Journal, Series A*, 44(4), 556-566, 2001.
- [19] Ou, Z. C., and Xijia, Wu., On the crack-tip stress singularity of interfacial cracks in transversely isotropic piezoelectric bimetals, *Int. J. of Solids and Structure*, 40, 7499-7511, 2003.